



# Tungstate-supported silica-coated magnetite nanoparticles: a novel magnetically recoverable nanocatalyst for green synthesis of nitroso arenes

Masoume Jadidi Nejad<sup>1</sup> · Elahe Yazdani<sup>1</sup> · Maryam Kazemi Miraki<sup>1</sup> · Akbar Heydari<sup>1</sup>

Received: 1 August 2018 / Accepted: 5 February 2019  
© Institute of Chemistry, Slovak Academy of Sciences 2019

## Abstract

Tungstate ion was heterogenized on the silica-coated magnetite nanoparticles and applied for the selective oxidation of anilines to nitroso arenes—with hydrogen peroxide/urea as oxidant in dimethyl carbonate as solvent—in moderate–good yields (40–96%). The catalyst was characterized using different techniques including Fourier-transform infrared spectroscopy, X-ray powder diffraction, vibrating sample magnetometry, scanning electron microscopy, energy dispersive X-ray and inductively coupled plasma atomic emission spectroscopy (ICP-AES). The catalyst was easily recovered using an external magnet and reused for six times.

**Keywords** Nitrosobenzene · Tungstate · Magnetite · Nano catalyst · Urea hydrogen peroxide

## Introduction

Nitroso compounds are versatile building blocks in polymer, dyes, agrochemicals and pharmaceutical industries (Biradar et al. 2008). Their easy preparation from inexpensive starting materials renders them cost-effective intermediates in synthetic organic chemistry (Hunger 2007). Furthermore, regioselective characteristics of nitroso compounds reactions, brings up a useful method for synthesis of natural-product simulated molecules (Huang et al. 2016).

Nitroso compounds are classically prepared by oxidation of anilines with various organic or inorganic oxidants (Defoin 2004; Priewisch and Rück-Braun 2005; Yost and Gutmann 1970; Di Nunno et al. 1970).

Catalyst-free methods include peracid oxidants, especially Caro acid, perbenzoic and peracetic acid (Bordoloi

and Halligudi 2007; Gowenlock and Richter-Addo 2004). However, reactions of these reagents are so violent which produce complex mixtures of over-oxidized, non-regio and chemoselective side products (Tayebie and Alizadeh 2007). To overcome these problems, catalytic strategies using milder oxidants such as aqueous hydrogen peroxide, *tert*-butyl peroxide and urea hydrogen peroxide (UHP) have been devised (Defoin 2004; Priewisch and Rück-Braun 2005; Yost and Gutmann 1970; Di Nunno et al. 1970). However, the composition of the obtained product mixture delicately depends on the nature and stoichiometry of the oxidant, reaction conditions like time and temperature and most importantly the nature of the catalyst used (Alizadeh and Tayebie 2005). The catalysts for amine oxidation can be classified into three classes, i.e., metallic ions such as ferrous, oxides (Croston et al. 2002) and complexes of metals like Mo, W, V, Zr and Re (Defoin 2004; Priewisch and Rück-Braun 2005; Yost and Gutmann 1970; Di Nunno et al. 1970), metal nanoparticles like Au (Fountoulaki et al. 2016) and surface-mediated catalysts like silicate-based molecular sieves (Reddy and Sayari 1994; Fields and Kropp 2000; Hosseini et al. 2018). Amongst these classes of catalysts, only molybdenum and tungstate are selective for nitroso compounds (Bordoloi and Halligudi 2007; Gowenlock and Richter-Addo 2004). Recently, tungstate-activated catalytic oxidations have received considerable interest due to their high activity and selectivity (Hosseini et al. 2018). However,

This article is dedicated to memory of Mahdi Zeinoddin.

**Electronic supplementary material** The online version of this article (<https://doi.org/10.1007/s11696-019-00708-x>) contains supplementary material, which is available to authorized users.

✉ Akbar Heydari  
heydar\_a@modares.ac.ir

<sup>1</sup> Chemistry Department, Tarbiat Modares University, P.O. Box 14155-4838, Tehran, Iran

**Scheme 1** Pathway to synthesis of FSW nanoparticles

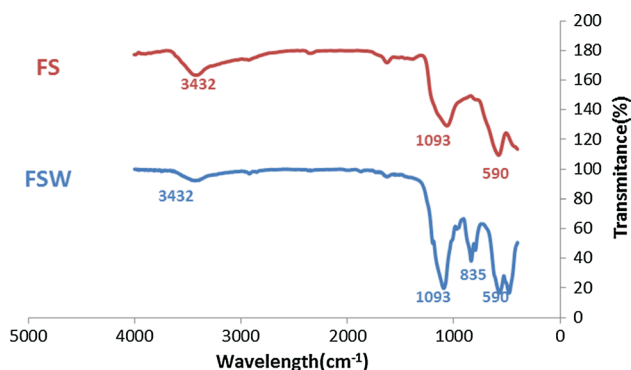
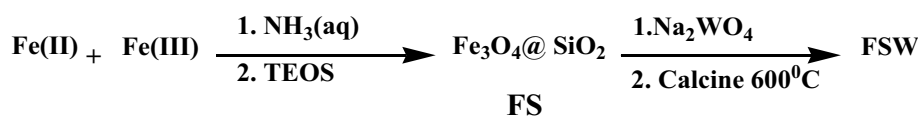


**Fig. 1** FT-IR spectra of FS and FSW nanoparticles

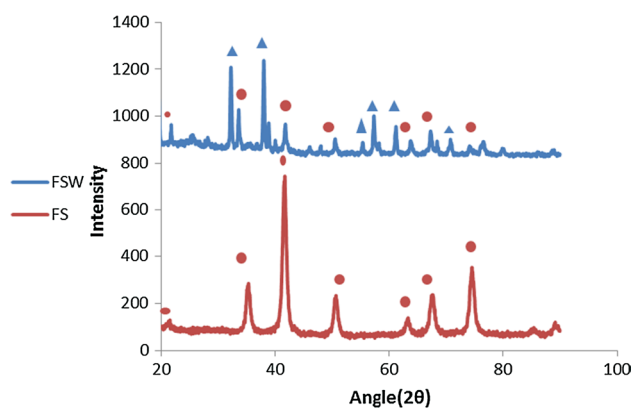


**Fig. 2** XRD patterns of FS and FSW nanoparticles

these systems lack enough efficiency for large-scale productions, due to cumbersome recycling of the catalyst and contamination of the final product either in homogeneous systems or solid supported ones (Hosseini et al. 2018; Hosseini Eshbala et al. 2017). In the present study, on the continuation of our on-going research on green organic synthesis, we introduce the application of magnetic nanoparticles supported tungstate as an efficient and easily recyclable nanocatalyst for selective oxidation of anilines to the corresponding nitroso compounds in dimethyl carbonate as the reaction media (Ma'mani et al. 2011). The importance of application of dimethyl carbonate as the reaction media is the enhanced solubility of organic substrates in this solvent as compared to water solubilities, as well as being a green and environmentally benign solvent.

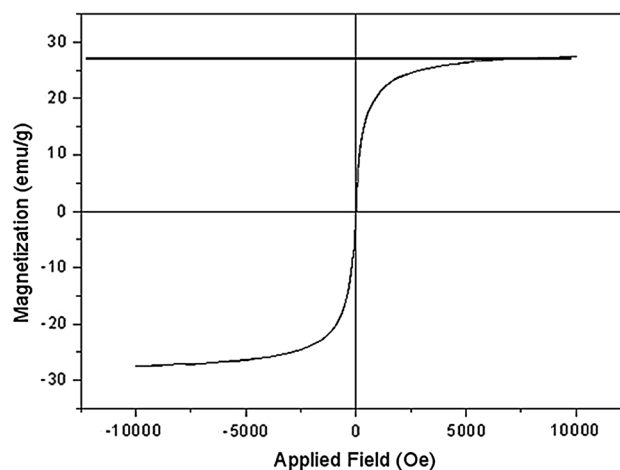


**Fig. 3** Vibrating sample magnetometry of FSW nanoparticles

## Experimental

All chemicals and solvents were of reagent grade and purchased from Merck and used without further purification. Amine derivatives were purchased from Sigma-Aldrich with reagent grade purity. FT-IR spectra were obtained over the region 400–4000  $\text{cm}^{-1}$  with a Nicolet IR100 FT-IR with spectroscopic grade KBr. X-ray powder diffraction (XRD) patterns were obtained at room temperature with a Philips X-pert 1710 diffractometer with  $\text{Co K}\alpha$  ( $\lambda = 1.78897 \text{ \AA}$ ), 40 kV voltage, 40 mA current and in the range 10–90° ( $2\theta$ ) with a scan speed of 0.020°  $\text{s}^{-1}$ . Scanning electron microscopy (SEM) (Philips XL 30 and S-4160) was used to study the catalyst morphology and size. Magnetic saturation of the catalyst was investigated using a vibrating magnetometer/alternating gradient force magnetometer (VSM/AGFM, MDK Co., Iran). ICP analysis was performed using a ICP-OES, Varian 730-ES instrument.  $^1\text{H}$  NMR spectra were recorded with a Bruker Avance (DRX 500 MHz, DRX 250 MHz) in pure deuterated chloroform solvent with tetramethylsilane as internal standard.

### Preparation of $\text{Fe}_3\text{O}_4@\text{SiO}_2\text{-NaWO}_4$ (FSW)

#### Preparation of silica-coated magnetite nanoparticles ( $\text{Fe}_3\text{O}_4@\text{SiO}_2$ )

Magnetite nanoparticles were prepared according to the previously reported literature (Liu et al. 2017). Separate

**Fig. 4** SEM image of **a** FS and **b** FSW nanoparticles

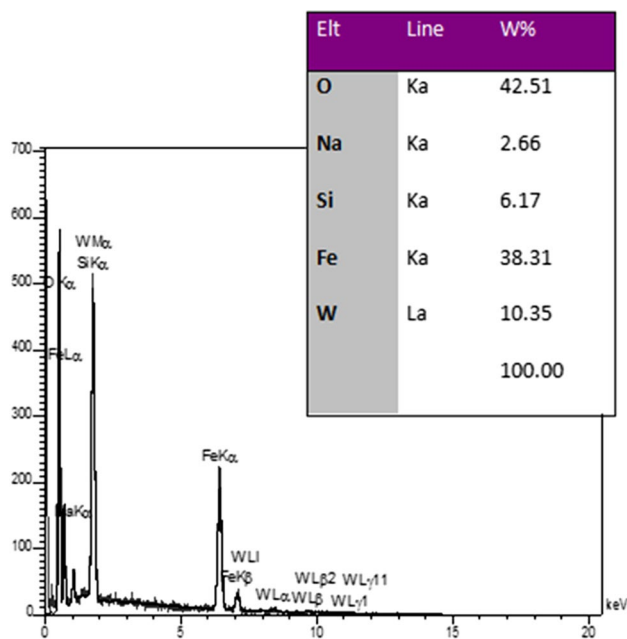
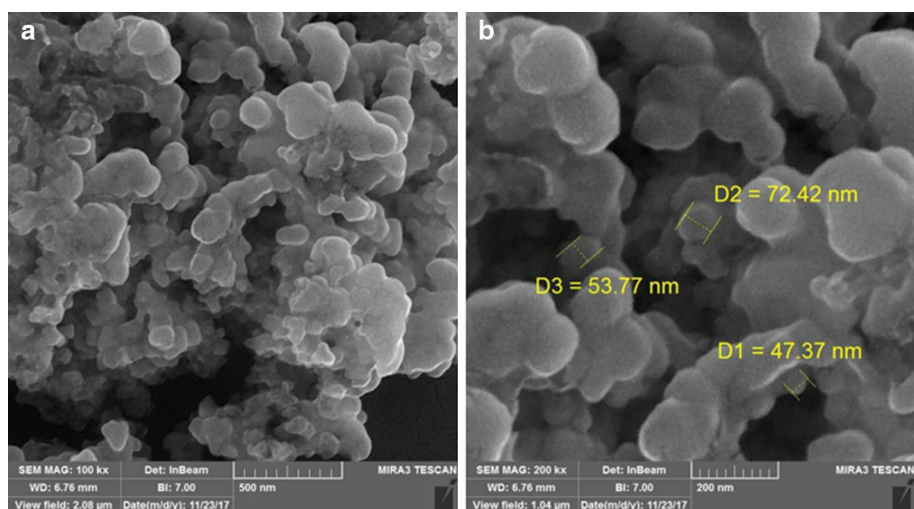


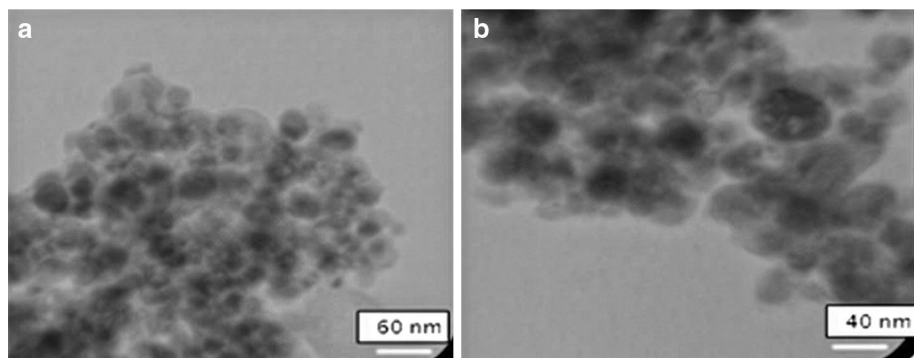
**Fig. 5** EDS analysis of FSW nanoparticles

solutions of 10 mmol  $\text{FeCl}_3 \cdot 6\text{H}_2\text{O}$  and 5 mmol  $\text{FeCl}_2 \cdot 4\text{H}_2\text{O}$  in 40 mL deionized water were mixed and vigorously stirred at 80 °C. Subsequently, 10 mL of aqueous ammonia solution (25%) was added in small portions to pH 11. After 2 h, 40 mL of EtOH and 5 mL of tetraethyl orthosilicate (TEOS) were added to the mixture in a stepwise manner. The resulting suspension was stirred mechanically for about 18 h at 40 °C. The resulting black solid was magnetically filtered and washed several times with water and EtOH and dried overnight at 60 °C.

#### Immobilization of tungstate on the surface of silica-coated magnetite nanoparticles

1 g of  $\text{Fe}_3\text{O}_4 @ \text{SiO}_2$  was dispersed in 50 mL of water with the aid of an ultrasonic bath. Then a solution of 1 mmol  $\text{Na}_2\text{WO}_4 \cdot 2\text{H}_2\text{O}$  in 50 mL water was added gradually to this dispersion. The mixture was vacuum dried using a rotary evaporator and calcined for 6 h at 60 °C.

**Fig. 6** TEM micrographs of **a** FS and **b** FSW nanoparticles



## General procedure for amine oxidation to nitroso arene

To a solution of 1 mmol amine in 2 mL DMC, was added 3 mmol UHP and 0.03 g catalyst. The mixture was stirred at room temperature for 2 h. Then the catalyst was removed using magnetic decantation. The reaction vessel was washed with water and extracted with dichloromethane ( $3 \times 10$  mL). The organic layer was dried with  $\text{Na}_2\text{SO}_4$  and the solvent was evaporated under vacuum. The crude product was purified using column chromatography if needed.

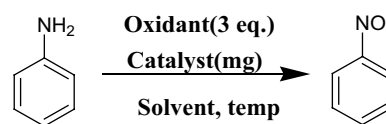
## Results and discussion

Scheme 1 shows the process of catalyst synthesis. The core-shell nanoparticles of  $\text{Fe}_3\text{O}_4@/\text{SiO}_2$  were prepared in the first step. Next, the tungstate moiety was linked to the shell during the calcination process. The resultant nanoparticles were characterized using different spectroscopic methods including Fourier-transform infrared spectroscopy (FT-IR), XRD, vibrating sample magnetometry (VSM), SEM-EDS and ICP analysis.

Variations in FT-IR spectrum of prepared final nanoparticles as compared to those of magnetite and silica-coated magnetite nanoparticles, proves the successful immobilization of tungstate moiety on the surface of the nanoparticles (Fig. 1). Peaks at  $3400\text{ cm}^{-1}$  can be ascribed to stretching vibrations of surface hydroxyl groups. Stretching vibrations of Si-O-Si groups appeared at around  $1090\text{ cm}^{-1}$ . Characteristic peaks of W-O and Fe-O bonds can be seen at  $590\text{ cm}^{-1}$  and  $835\text{ cm}^{-1}$ , respectively (Khoshnavazi et al. 2017; Habibi-Yangjeh and Shekofteh-Gohari 2017).

X-ray diffraction pattern of the prepared nanoparticles is illustrated in Fig. 2. The reported reference peaks of magnetite, i.e., 21.38, 35.27, 41.62, 50.71, 63.28, 67.64 and  $74.6^\circ$  corresponding to crystalline faces of (111), (220), (311), (400), (422), (511) and (440) are observed in the pattern demonstrating the crystalline purity of the particles core (Kazemi Miraki et al. 2017). A broad band at about  $30^\circ$  is demonstrative of silica shell. The new assigned bands are due to immobilized tungstate groups (Yildiz et al. 2014; Yan et al. 1992) which is in accordance with FT-IR findings. The bands observed at diffraction angles ( $2\theta$ ) of  $32.1$ ,  $37.9$ ,  $50.5$ ,  $57.3$ ,  $61.1$  and  $76.5^\circ$  are corresponding to sodium tungstate crystalline faces of (220), (311), (331), (422), (511) and (620) respectively (JCPD car no. 12-722).

Hysteresis loop of the prepared nanoparticles is reversible, with no remanence and saturation magnetization of  $28\text{ emu g}^{-1}$  in the applied magnetic field of  $-10,000$  to  $+10,000$  Oersted (Fig. 3). These results are indicative of superparamagnetic character of nanoparticles resulting in easy separation from reaction mixture using an external



**Scheme 2** Oxidation of aniline to nitrosobenzene

**Table 1** Optimization of reaction conditions of aniline oxidation

Entry	Catalyst (mg)	Oxidant	Solvent	Temp. ( $^\circ\text{C}$ )	Yield <sup>a</sup> (%)
1	0.03	UHP	DMF	r.t.	–
2	0.03	UHP	DMSO	r.t.	–
3	0.03	UHP	THF	r.t.	20
4	0.03	UHP	<i>n</i> -Hexane	r.t.	40
5	0.03	UHP	$\text{CHCl}_3$	r.t.	55
6	0.03	UHP	$\text{CH}_2\text{Cl}_2$	r.t.	50
7	0.03	UHP	$\text{CH}_3\text{OH}$	r.t.	60
8	0.03	UHP	$\text{CH}_3\text{CH}_2\text{OH}$	r.t.	55
9	0.03	UHP	$\text{CH}_3\text{CN}$	r.t.	50
10	0.03	UHP	$\text{H}_2\text{O}$	r.t.	75 <sup>b</sup> , 20 <sup>c</sup>
<b>11</b>	<b>0.03</b>	<b>UHP</b>	<b>DMC</b>	<b>r.t.</b>	<b>90</b>
12	0.03	$\text{H}_2\text{O}_2$	DMC	r.t.	70
13	0.03	Oxone	DMC	r.t.	50
14	0.03	TBHP	DMC	r.t.	–
15	0.03	UHP	DMC	60	50
16	0.03	UHP	DMC	90	40
17	0.02	UHP	DMC	r.t.	82
18	0.05	UHP	DMC	r.t.	93
19	–	UHP	DMC	r.t.	–
20	0.03 <sup>d</sup>	UHP	DMC	r.t.	–
21	0.03 <sup>e</sup>	UHP	DMC	r.t.	–

Reaction conditions: amine (1 mmol), oxidant (3 mmol), solvent (2 mL), 2 h

<sup>a</sup>Isolated yield

<sup>b</sup>Nitroso benzene product

<sup>c</sup>Nitrobenzene product

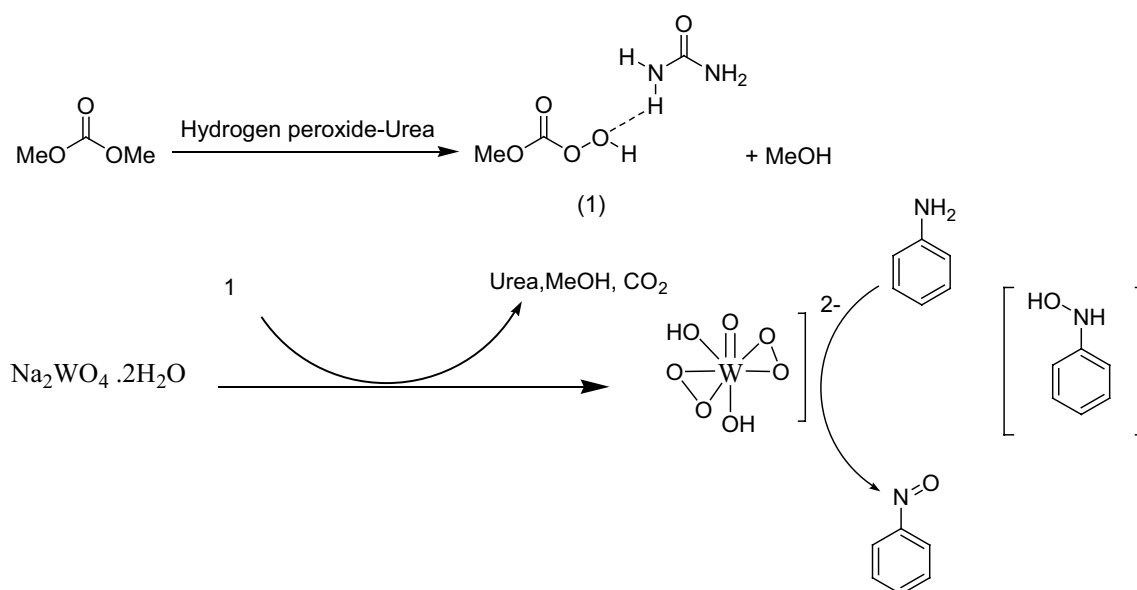
<sup>d</sup> $\text{Fe}_3\text{O}_4$  nanoparticles

<sup>e</sup> $\text{Fe}_3\text{O}_4@/\text{SiO}_2$  nanoparticles

permanent magnet. The relatively low amount of saturation magnetization as compared to bare magnetite nanoparticles ( $73\text{ emu g}^{-1}$ ) is due to silica coating and tungstate moieties as well (Ghonchepour et al. 2017).

SEM image of nanoparticles (FS and FSW) is depicted in Fig. 4. The morphology was evaluated to be almost spherical in shape. No considerable change in the morphology was observed after functionalization.

Energy dispersive X-ray (EDS) spectroscopy was performed to speculate the atomic composition of prepared nanoparticles (Fig. 5). Fe, Si and O are attributed to iron



**Scheme 3** Reaction pathway of oxidation of aniline to nitrosobenzene

oxide core and silica shell of nanoparticles and W and Na peaks are totally related to tungstate-immobilized groups. The percentage of tungsten element observed in the EDS table, is equivalent to 0.563 mmol of this element in 1 g of the final nanoparticles; while EDS results are not quantitatively reliable, as it is a surface probe, the precise amount of tungsten element was determined using inductively couple plasma (ICP) analysis. The results showed the presence of 0.557 mmol of tungsten per gram of nanoparticles.

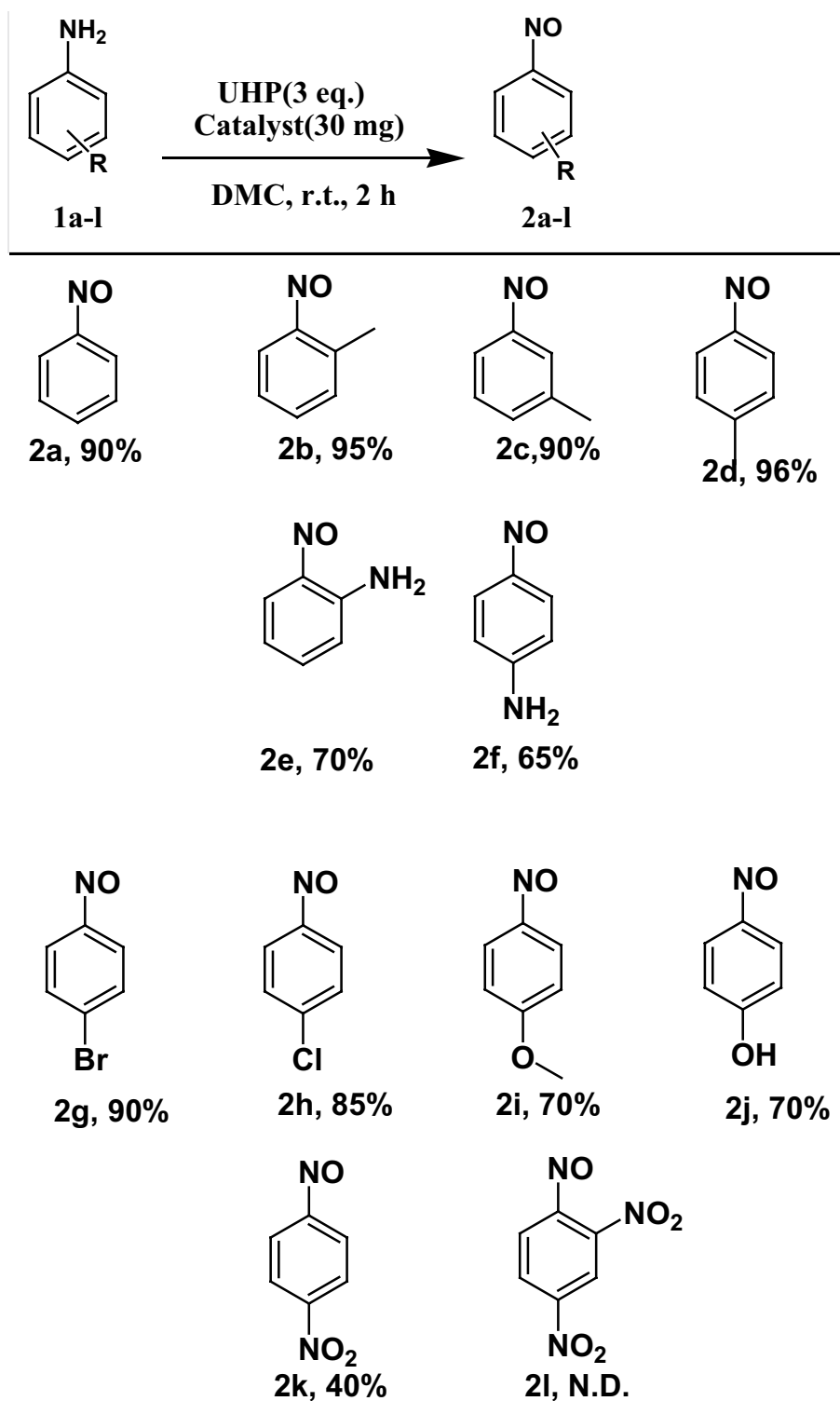
Transmission electron micrographs of FS and FSW nanoparticles are shown in Fig. 6. Core-shell nature of both nanoparticles is observable.

After characterization of nanoparticles, their catalytic activity was examined in selective oxidation of aniline to the nitroso benzene as a model reaction (Scheme 2). The optimized reaction condition was studied and the results are outlined in Table 1. Initially, the effect of solvent was surveyed in the formation of nitroso benzene while the oxidant (UHP) applied, was kept constant (entries 1–11). In DMF and DMSO no product formation was observed (entries 1–2). Considerably, low product yield was obtained in THF (entry 3). The yield of product was moderate in alkane, chlorinated solvents, alcohols and acetonitrile (entries 4–9). The reaction in water was not so selective and 20% of nitro product was observed (entry 10). The oxidation reaction was efficient and highly selective for nitroso product in dimethyl carbonate as solvent (entry 11). It can be suggested that, polar protic solvents, i.e., water and alcohols promote the reaction by easy dissolution of oxidant (UHP), while non-polar solvents dissolve the amine substrate which result in comparable product yield in spite of low solubility of oxidant. Hence the product

yields do not largely depend to solvent polarity. However, DMC plays a different role in the reaction which is shown in the reaction mechanism (Scheme 3). With the optimized solvent in hand, various oxidants were tested in the model reaction (entries 12–14). Using hydrogen peroxide and oxone as oxidant, lower product yields were obtained; surprisingly when *tert*-butyl hydrogen peroxide was applied, no product was detected (entry 14). The efficiency of the oxidation reaction using DMC as solvent and UHP as oxidant in elevated temperatures were tested (entries 15–16). It was observed that at higher temperatures formation of nitro compounds precedes over nitroso formation. In addition, effect of lower and higher amount of catalyst was studied (entries 17–18). As it was expected, no product was detected in the absence of the catalyst (entry 19). Furthermore, reaction did not proceed when magnetite and silica-coated magnetite nanoparticles were used as catalyst (entries 20–21). Overall, DMC and UHP at ambient temperature were much more selective for production of nitroso compound in excellent yields.

After achieving the best reaction condition, substrate scope of the reaction was surveyed. For electron donating substituents like methoxy, hydroxy and amino group moderately good yields of corresponding nitroso compound was obtained (**2e–f**, **2i–j**); while for electron withdrawing groups like Cl, Br and nitro product yield was diminished (**2g–h** and **2k**). Even though for double nitro substituted amine, no product formation was detected (**2l**). Where two amino groups were present in the starting material, the protocol was selective to oxidation of only one and no over or di-oxidated product was observed (**2e–f**) (Table 2).

**Table 2** FSW catalyzed oxidation of anilines to corresponding nitroso arenes



Reaction conditions: amine (1 mmol), UHP (3 mmol), catalyst (30 mg), DMC (2 mL), room temperature, 2 h

Isolated yield

A reaction pathway of amine oxidation to nitroso arene in the presence of supported tungstate catalyst is depicted in Scheme 3. Initially, tungstate is converted to corresponding peroxy ion through reaction with UHP (Strukul 2013)

and hydroxyl amine is produced as an intermediate. When hydroxyl amine undergoes the same reaction, the desired product of nitroso arene is formed. The role of dimethyl carbonate as solvent is the ultimate activation of UHP; first

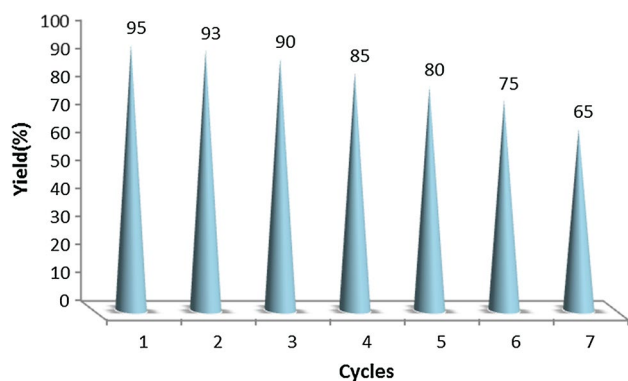


Fig. 7 Recycling of FSW in the oxidation of aniline to nitrosobenzene

it is converted to its corresponding peroxide with liberation of methanol. Then urea activates the resulting peroxide via hydrogen bonding (Kraïem et al. 2016).

Reusability of the prepared catalyst was evaluated in the model reaction. After the reaction was considered completed, the catalyst was separated from the reaction mixture with the aid of a permanent external magnet. Then it was

consecutively washed three times with dichloromethane, methanol and acetone, dried at ambient temperature and the vessel was charged with reagents to react for the next run. This process was repeated for 6 cycles with negligible decrease in the catalyst activity (Fig. 7). Furthermore, ICP analysis of the reaction mixture indicated no leaching of tungstate from the catalyst support.

The recycled catalyst was characterized after sixth run and it showed no significant changes in its structure (Fig. 8).

Because most of the products have been characterized, analytical identification of the synthesized adducts is limited to the infrared, MS and melting point for some products. Spectral data for selected derivatives:

**3-Methylnitrosobenzene (2c)** Dark yellow solid; 90% yield; mp: 65–67 °C; IR (KBr)  $\nu$  (cm<sup>-1</sup>) = 3110, 2923, 1614, 1456, 1261, 1107, 753, 624. <sup>1</sup>H NMR (500 MHz, CDCl<sub>3</sub>):  $\delta$  3.34 (s, 3H), 6.27 (dd,  $J$  = 1.02–8.15 Hz, 1H), 7.15 (t,  $J$  = 7.6 Hz, 1H), 7.53 (td,  $J$  = 7.65–0.65, 1H), 7.58 (dt,  $J$  = 1.4–7.65, 1H).

**2-Aminonitrosobenzene (2e)** Green solid; 70% yield; mp: 80–82 °C; IR (KBr)  $\nu$  (cm<sup>-1</sup>) = 3386, 2922, 2360, 1624,

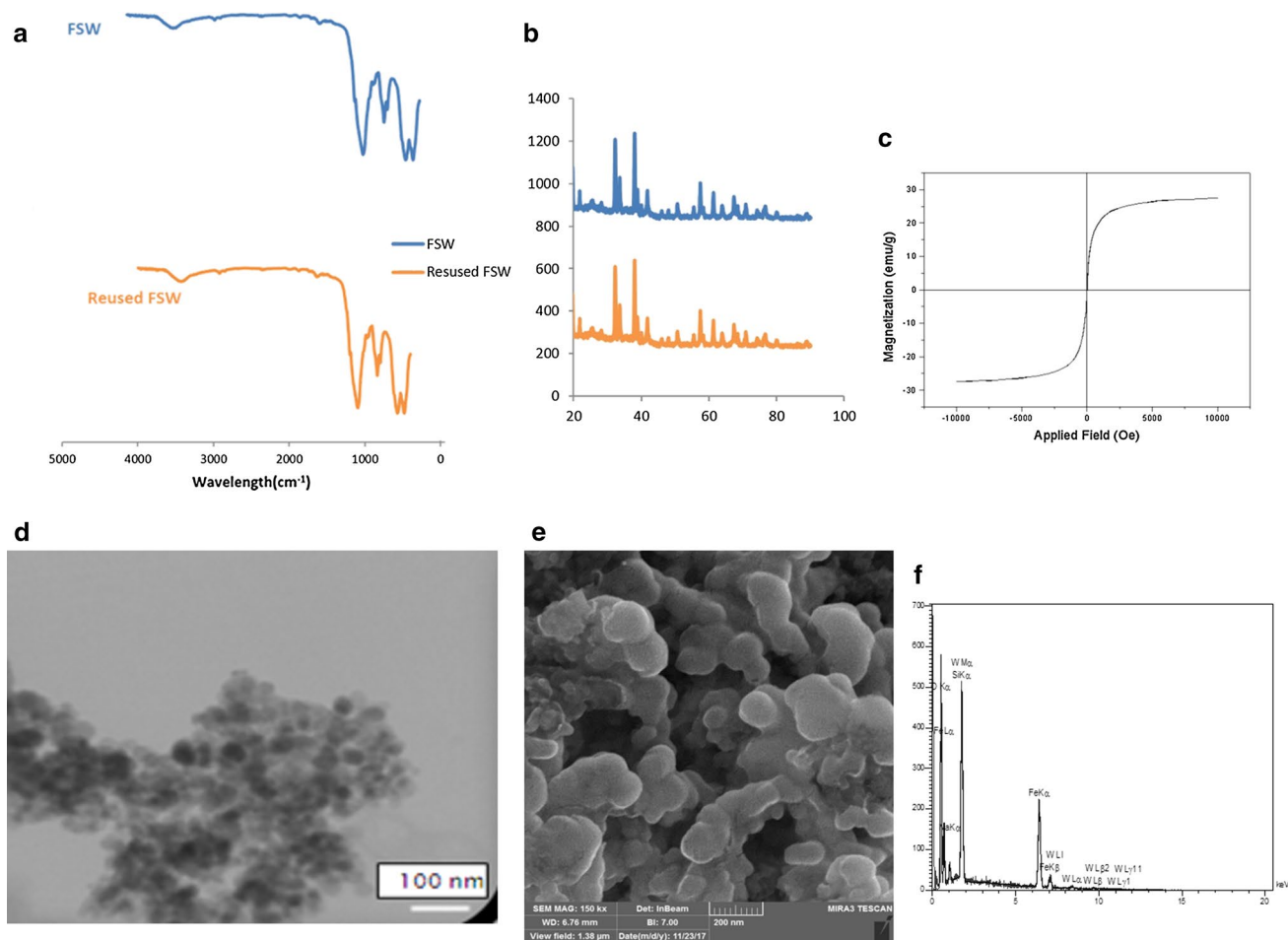


Fig. 8 a FT-IR, b XRD, c VSM, d TEM, e SEM and f EDS of recycled FSW (after 6th run)

1504, 1347, 1254, 1105, 1024, 745. MS (EI, 70 eV):  $m/z$  (%) = 122 (M+, 100), 92 (78), 90 (13), 76 (10), 75 (9), 65 (82), 63 (15), 52 (14).

$^1\text{H NMR}$  (500 MHz,  $\text{CDCl}_3$ ):  $\delta$  6.95 (t,  $J = 7.8$  Hz, 2H), 7.35 (dd,  $J = 7.65$ –1.3, 2H), 8.68 (s, 2H).

**4-Aminonitrosobenzene (2f)** Dark green solid; 65% yield; mp: 146–148 °C; IR (KBr)  $\nu$  ( $\text{cm}^{-1}$ ) = 3354, 2924, 1657, 1614, 1600, 1510, 1327, 1286, 1236, 1103, 834, 632. MS (EI, 70 eV):  $m/z$  (%) = 122 (M+, 100), 92 (62), 85 (11), 71 (19), 65 (61), 57 (21).

$^1\text{H NMR}$  (500 MHz,  $\text{CDCl}_3$ ):  $\delta$  4.38 (s, 2H), 6.62 (d,  $J = 9.05$  Hz, 2H), 8.07 (d,  $J = 9.05$  Hz, 2H).

**4-Nitronitrosobenzene (2k)** Pale yellow solid, 40% yield; mp: 185–187 °C; IR (KBr)  $\nu$  ( $\text{cm}^{-1}$ ) = 3416, 2923, 1624, 1549, 1343, 1107, 756.  $^1\text{H NMR}$  (500 MHz,  $\text{CDCl}_3$ ):  $\delta$  7.26 (s, 2H), 8.42 (s, 2H).

## Conclusions

Sodium tungstate-supported magnetite nanoparticles were prepared and characterized. The catalytic activity of the nanoparticles was screened in the selective oxidation of anilines to the corresponding nitroso arenes in good yields using urea/hydrogen peroxide oxidant, in dimethyl carbonate as a green reaction media. The method showed acceptable tolerance to electron donating and withdrawing substituents. The catalyst was easily recovered with the magnetic power and reused for 6 cycles; although a relatively significant drop in product yield was observed after 6 cycles, it can be considered acceptable to a large extent. Hence this catalytic system brings up a new vision in the selective catalytic oxidation of anilines to corresponding nitroso compounds.

**Acknowledgements** We acknowledge Tarbiat Modares University for partial support of this.

## References

- Alizadeh M, Tayeb R (2005) Catalytic oxidation of aniline by aqueous hydrogen peroxide in the presence of some heteropolyoxometalates. *J Braz Chem Soc* 16:108–111. <https://doi.org/10.1590/S0103-50532005000100017>
- Biradar AV, Kotbagi TV, Dongare MK, Ubmarkar SB (2008) Selective N-oxidation of aromatic amines to nitroso derivatives using a molybdenum acetylido oxo-peroxo complex as catalyst. *Tetrahedron Lett* 49:3616–3619. <https://doi.org/10.1016/j.tetlet.2008.04.005>
- Bordoloi A, Halligudi SB (2007) Tungsten- and molybdenum-based coordination polymer-catalyzed N-oxidation of primary aromatic

- amines with aqueous hydrogen peroxide. *Adv Synth Catal* 349:2085–2088. <https://doi.org/10.1002/adsc.200700224>
- Croston M, Langston J, Takacs G, Morrill TC (2002). <http://scholarworks.rut.edu/other/472>
- Defoin A (2004) Simple preparation of nitroso benzenes and nitro benzenes by oxidation of anilines with  $\text{H}_2\text{O}_2$  catalysed with molybdenum salts. *Synthesis* 5:706–710
- Di Nunno L, Florio S, Todesco PE (1970) Oxidation of substituted anilines to nitroso-compounds. *J Chem Soc C* 10:1433–1434. <https://doi.org/10.1039/J39700001433>
- Fields JD, Kropp PJ (2000) Surface-mediated reactions. 9. Selective oxidation of primary and secondary amines to hydroxylamines. *J Org Chem* 65:5937–5941. <https://doi.org/10.1021/jo0002083>
- Fountoulaki S, Gkizis PL, Symeonidis TS, Kaminioti E, Karina A, Tamiolakis I, Armatas S, Lykakis IN (2016) Titania-supported gold nanoparticles catalyze the selective oxidation of amines into nitroso compounds in the presence of hydrogen peroxide. *Adv Synth Catal* 358:1500–1508. <https://doi.org/10.1002/adsc.20150957>
- Ghonchepour E, Yazdani E, Saberi D, Arefi M, Heydari A (2017) Preparation and characterization of copper chloride supported on citric acid-modified magnetite nanoparticles ( $\text{Cu}^{2+}$ -CA@ $\text{Fe}_3\text{O}_4$ ) and evaluation of its catalytic activity in the reduction of nitroarene compounds. *Appl Organomet Chem* 31:e3822. <https://doi.org/10.1002/aoc.3822>
- Gowenlock BG, Richter-Addo GB (2004) Preparations of C-nitroso compounds. *Chem Rev* 104:3315–3340. <https://doi.org/10.1021/cr030450k>
- Habibi-Yangjeh A, Shekofteh-Gohari M (2017) Novel magnetic  $\text{Fe}_3\text{O}_4/\text{ZnO}/\text{NiWO}_4$  nanocomposites: enhanced visible-light photocatalytic performance through p-n heterojunctions. *Sep Purif Technol* 184:334–346. <https://doi.org/10.1016/j.seppur.2017.05.007>
- Hosseini Eshbala F, Mohanazadeh F, Sedrpoushan A (2017) Tungstate ions ( $\text{WO}_4^{2-}$ ) supported on imidazolium framework as novel and recyclable catalyst for rapid and selective oxidation of benzyl alcohols in the presence of hydrogen peroxide. *Appl Organomet Chem* 32:3597. <https://doi.org/10.1002/aoc.3597>
- Hosseini SH, Tavakolizadeh M, Zohreh N, Soleyman R (2018) Green route for selective gram-scale oxidation of sulfides using tungstate/triazine-based ionic liquid immobilized on magnetic nanoparticles as a phase-transfer heterogeneous catalyst. *Appl Organomet Chem* 32:e3953. <https://doi.org/10.1002/aoc.3953>
- Huang J, Chen Z, Yuan J, Peng Y (2016) Recent advances in highly selective applications of nitroso compounds. *Asian J Org Chem* 5:951–960. <https://doi.org/10.1002/ajoc.201600242>
- Hunger K (2007) Industrial dyes: chemistry, properties, applications. Wiley, New York, pp 110–112
- Kazemi Miraki M, Yazdani E, Ghandi L, Azizi K, Heydari A (2017) Mild and eco-friendly chemoselective acylation of amines in aqueous medium using a green, superparamagnetic, recoverable nanocatalyst. *Appl Organomet Chem* 31:e3744. <https://doi.org/10.1002/aoc.3744>
- Khoshnavazi R, Bahrami L, Rezaei M (2017) Heteropolytungstostannate as a homo- and heterogeneous catalyst for Knoevenagel condensations, selective oxidation of sulfides and oxidative amination of aldehydes. *RSC Adv* 7:45495–45503. <https://doi.org/10.1039/C7RA06112A>
- Kraiem J, Ghedira D, Ollevier T (2016) Hydrogen peroxide/dimethyl carbonate: a green system for epoxidation of N-alkylimines and N-sulfonylimines. One-pot synthesis of N-alkyloxaziridines from N-alkylamines and (hetero) aromatic aldehydes. *Green Chem* 18:4859–4864. <https://doi.org/10.1039/C6GC01394E>
- Liu L, Ai Y, Li D, Qi L, Zhou J, Tang Z, Shao Z, Liang Q, Sun HB (2017) Recyclable acid-base bifunctional core-shell-shell nanoparticle catalyzed synthesis of 5-aryl-NH-1,2,3-triazoles via “one-pot” cyclization of aldehyde, nitromethane and  $\text{NaN}_3$ .



- ChemCatChem 16:3131–3137. <https://doi.org/10.1002/cctc.201700401>
- Ma'mani L, Sheykhan M, Heydari A (2011) Nanosilver embedded on hydroxyapatite-encapsulated Fe<sub>2</sub>O<sub>3</sub>: superparamagnetic catalyst for chemoselective oxidation of primary amines to *N*-monoalkylated hydroxylamines. *Appl Catal A* 395:34–38. <https://doi.org/10.1016/j.apcata.2011.01.015>
- Priewisch B, Rück-Braun K (2005) Efficient preparation of nitrosoarenes for the synthesis of azobenzenes. *J Org Chem* 70:2350–2355. <https://doi.org/10.1021/jo048544x>
- Reddy JS, Sayari A (1994) Oxidation of primary amines over vanadium silicalite molecular sieve, VS-1. *Catal Lett* 28:263–267. <https://doi.org/10.1007/BF00806055>
- Strukul G (2013) Catalytic oxidations with hydrogen peroxide as oxidant. Springer Science & Business Media, Berlin, pp 187–191
- Tayeb R, Alizadeh MH (2007) Water as an efficient solvent for oxygenation transformations with 34% hydrogen peroxide catalyzed by some heteropolyoxometalates. *Monatsh Chem* 138:763–769. <https://doi.org/10.1007/s00706-007-0660-z>
- Yan QJ, Wang Y, Jin YS, Chen Y (1992) Methane oxidative coupling over Na<sub>2</sub>WO<sub>4</sub>/SiO<sub>2</sub>. *Catal Lett* 13:221–228. <https://doi.org/10.1007/BF00770994>
- Yildiz M, Aksu Y, Simon U, Kailasam K, Goerke O, Rosowski F, Arndt S (2014) Enhanced catalytic performance of Mn<sub>x</sub>O<sub>y</sub>-Na<sub>2</sub>WO<sub>4</sub>/SiO<sub>2</sub> for the oxidative coupling of methane using an ordered mesoporous silica support. *Chem Comm* 50:14440–14442. <https://doi.org/10.1039/C4CC06561A>
- Yost Y, Gutmann HR (1970) Hindered *N*-arylhydroxamic acids from arylamines via nitroso-compounds. *J Chem Soc C* 18:2497–2499. <https://doi.org/10.1039/J39700002497>

**Publisher's Note** Springer Nature remains neutral with regard to jurisdictional claims in published maps and institutional affiliations.